Penerbit Akademia Baru

Journal of Advanced Research in Fluid Mechanics and Thermal Sciences

Journal homepage: www.akademiabaru.com/arfmts.html
ISSN: 2289-7879

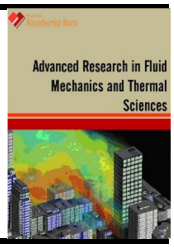

Flow Past Two Interlocking Squares Cylinder at Low Reynolds Number

Open Access

Muhamad Hafiz Md Jamal[1], Azlin Mohd Azmi[1,*]

[1] Faculty of Mechanical Engineering, Universiti Teknologi MARA, 40450 Shah Alam Selangor, Malaysia

ARTICLE INFO

Article history:
Received 18 March 2018
Received in revised form 6 April 2018
Accepted 28 April 2018
Available online 30 April 2018

Keywords:
Passive control, Screen mesh, Shroud, Vortex shedding

ABSTRACT

Flow past two interlocking squares cylinder is largely unexplored in the field of bluff body wake. This paper aims to investigate the wake region behind this body at *Re*=150. The study was carried out numerically using ANSYS-Fluent solver with viscous-laminar model. The results obtained were compared with that of a square cylinder. It was observed that the flow separation was delayed at the downstream sharp corner of the two interlocking squares cylinder, resulting in an early interaction between the shear layers behind its wake. The maximum vorticity magnitude was slightly higher (of about 6%), indicating a higher intensity of vortices in the two interlocking squares wake than that of the square cylinder wake, consistent with the spectral analysis. A larger lift fluctuation with higher amplitude was also observed in the former in comparison to that in the latter.

1. Introduction

Flow over bluff bodies have been the subject of studies in the last decades through both numerical and experimental method due to its importance and wide application in engineering applications. The wake of a bluff body is complex as it involves the interactions of three shear layers namely a boundary layer, a separating free shear layer, and a wake region [1]. At a critical Reynold numbers, the flow produces vortex shedding in the wake region, resulting from the boundary layer separation due to an adverse pressure gradient. This can sometimes lead to unwanted structural vibrations when the vortex shedding frequency matches the resonance frequency of the structure (lock in), a phenomenon called vortex-induced vibration (VIV). Most bluff body studies have been dedicated to examine the unsteady nature behind the body and the effects on flow-induced vibrations.

A circular cylinder and square cylinder have been extensively investigated in the past and were mainly considered as baseline bodies in many applications [2, 3]. For a square cylinder, the flow separation takes place at the upstream sharp corners, which produces a large drag force due to

* *Corresponding author.*
E-mail address: azlinma@gmail.com (Azlin Mohd Azmi)

formation of a wide wake behind the cylinder [4]. As the square cylinder has pointed shape and flat surface, the drag force acted on it is higher than that of a circular cylinder. The study also showed that a square cylinder with rounded corners effectively reduced the drag and lift forces generated behind the cylinder. A study on vortex shedding behind a porous square cylinder showed that vortex occurs early in the wake with longer shedding period for low porosity cylinder [5]. Flow past a square cylinder at an angle of incidence was also explored [6, 7], with results indicated that the overall wake properties depended on the cylinder orientation. Flow over hybrid bodies such as those of a square cylinder attached with extended triangular solid (thorn) [8] and a square cylinder with an attached splitter plate were also investigated [9] for drag reduction and flow control effects.

In recent years, many energy harvesting devices based on VIV have been explored and developed exhaustively to take advantage of the periodic vortices formed behind a body [10, 11]. These irregular vortices induce motions on the body which will convert the flow energy into mechanical energy. The body that is widely used is a circular cylindrical body. The power generated by a body driven by VIV is a function of oscillation amplitude and frequency. Thus, it is vital to explore a different geometry that will maximize the VIV to provide a greater power output. A two-interlocking squares cylinder with its many sharp corners may have that advantage of greater power output due to large oscillation amplitudes. This body consists of two overlapping squares with one square titled over the other to form an eight-pointed star. In addition, this body has been adopted as the cross section of the Petronas Twin Tower structure, resembling the motif of Rub el Hizb [12], but no studies have been documented on its wake dynamics.

Motivated by the above, the present study aims to examine the wake behind the two interlocking squares cylinder by analyzing the time-averaged fluctuating forces, Strouhal number and the flow contours and comparing the results with that of a square cylinder. To the author's knowledge, there has been no investigation on the flow behind this body. It is imperative to have a good understanding of the flow field behind this body and its unsteady effects to exploit its engineering potential. A low Reynolds number of 150 is chosen for the preliminary work.

2. Methodology

The study was first done by validating the simulation results for flow over a square cylinder with that of existing experimental data. The Strouhal number and the drag coefficient between the experimental and simulation work of the square cylinder is in very good agreement with each other with difference of about 1% to 9% as shown in Table 1. The result from the simulation for flow over two interlocking square is then compared with the data from the square cylinder with the same computational setup.

Table 1
Drag Coefficient and Strouhal Number at *Re*=150

Shape		Drag Coefficient, C_d	Strouhal Number, St
Square Cylinder	Robichaux, et al. [13]	-	0.165
	Inoue, et al. [14]	1.40	0.151
	Doolan [15]	1.44	0.156
	Ali, et al. [16]	1.47	0.160
	Present study	1.41	0.150
Two interlocking squares		1.34	0.180

Figure 1 shows the two interlocking squares geometry and the rectangular computational domain. The ratio, *D/B* was set as 1. The two interlocking squares was placed at 23D and 40D, respectively from the cylinder axis. The top and bottom boundaries were both located at 25D from the cylinder axis. These values were used to minimize the effect of boundaries and to adequately meet the free stream condition. A structured form mesh with 140658 cells was employed for the computational process as shown in Fig. 2.

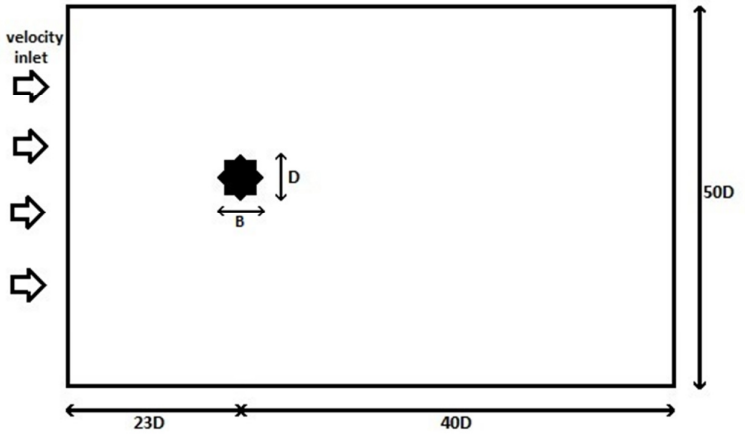

Fig. 1. Geometry of two interlocking squares and the flow computational domain

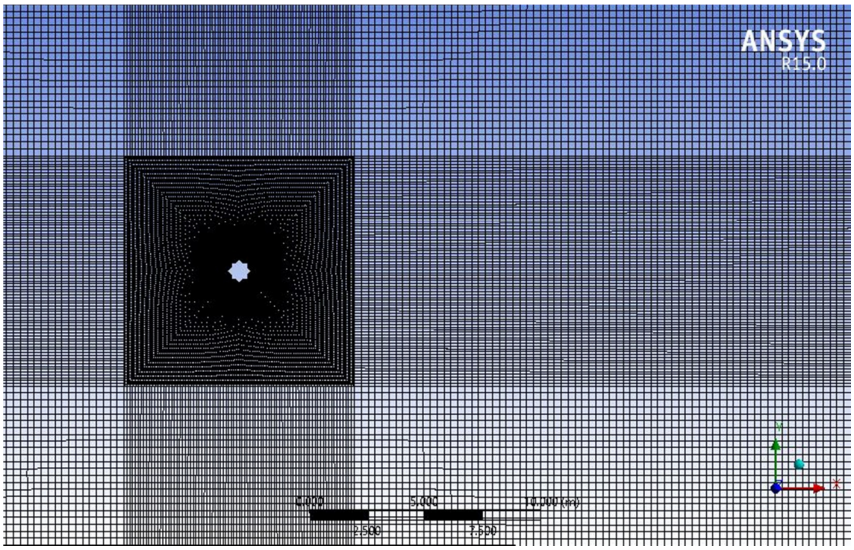

Fig. 2. Structured mesh around interlocking squares

The viscous laminar model in transient time was used to simulate the unsteady flow at *Re*=150. No-slip condition and stationary wall boundary conditions were set at both walls and interlocking squares. Second order implicit solution method was used in the computational simulation. The calculation step of the simulation was initialized by hybrid initialization where the calculation was run at time step size of 0.001s for 1500 number of time step with 100 maximum iterations per time step in order to capture the flow structure in the wake region of the two interlocking squares.

The grid independency study was conducted to increase the numerical accuracy of the computed result and also to minimize the discretization error. The study was done by increasing the numbers of cells and nodes of the mesh around the two interlocking squares as shown in Table 2. Further grid refinement shows that the results for Strouhal number and drag of mesh M3 were sufficient, thus mesh M3 was used for this simulation.

Table 2
Grid information

Mesh	Nodes	Cells	Drag Coefficient, C_d	Strouhal Number, St
M1	9450	9232	0.97	0.16
M2	35873	35450	1.22	0.18
M3	141501	140658	1.34	0.18
M4	318938	317672	1.34	0.18

3. Results and discussions

Figure 3 shows the time history of the coefficient of drag and lift, C_d and C_l, respectively in the two wakes. Both profiles show the periodic sinusoidal nature of the flow signifying the presence of correlated vortex shedding. It can be observed that the interlocking squares wake reaches a "steady" state earlier than the square cylinder wake where the oscillation is stabilized until around 0.5 seconds into the run. At this point, the C_l amplitude remains fairly constant at a value of 0.5, higher than that produced by the square cylinder of 0.3.

Figure 4 shows the Spectral Analysis of Lift Convergence where it can be seen that both cylinder displays sharp peak to indicate the presence of regular periodic vortex shedding in the wake region. The Strouhal number which corresponds to the main shedding frequency is obtained from the maximum peak. The Strouhal number for the two interlocking squares cylinder is 0.18, 20% higher than that of the square cylinder of 0.15. It can be observed that the magnitude of the power spectral density for the two interlocking squares cylinder is considerably higher than that of the square cylinder implying a much higher intensity of vortices in the former in comparison to that in the latter.

The surface pressure coefficient is presented in Fig. 5. The pressure coefficient is defined as $C_p = (p - p_\infty)/0.5\rho U_\infty$, where p is the time-averaged pressure and p_∞ and U_∞ is the static pressure and velocity of the free stream, respectively. The pressure coefficient for the square cylinder drops from 0° to 45° and then recovers gradually thereafter. In contrast, the recovery region occurs twice for the interlocking squares; between 45° to 80° and 90° to 180°. The adverse pressure region causes the fluid particles to move away from the surface where the boundary layer starts to separate, a condition when the shear stress is equal to zero as depicted in Fig. 6. It can be seen that for the square cylinder, the flow starts to separate at 64° while for the two interlocking squares, the flow separates at 100° (the first recovery region is not significant enough to cause flow separation). Note also, the base pressure is slightly higher in the former than that in the latter.

Figure 7 shows the pressure coefficient contours for the square cylinder and two interlocking squares cylinder respectively. It is clearly shown that for both cases the pressure contour is asymmetric. There is a region of high pressure at the leading edge (stagnation point) and region of low pressure downstream of both bodies. However, the two interlocking squares cylinder wake region have higher maximum concentration of negative contour, marked by the deep blue shade, in comparison to the square cylinder, marked by turquoise. These blueish shades clearly indicate the

location and intensity of the vortices. The "old" vortex that formed moments before in the square cylinder wake quickly fades into the greenish shade whereas it is still blueish in the interlocking squares cylinder wake suggesting higher intensity of vortices in the latter in contrast to the former.

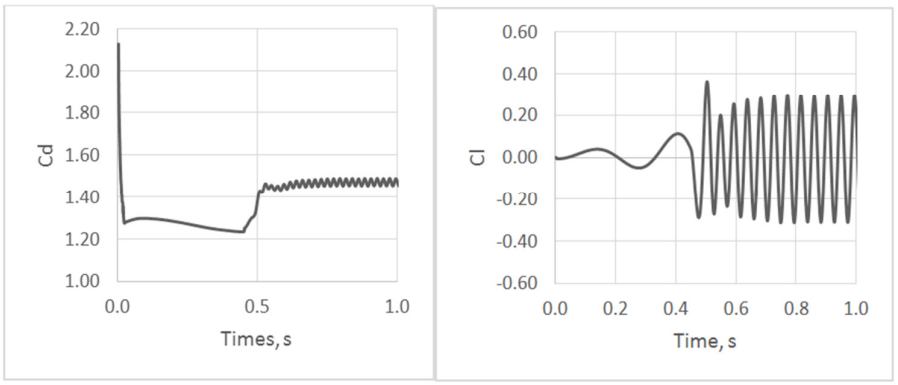

(a) Square Cylinder

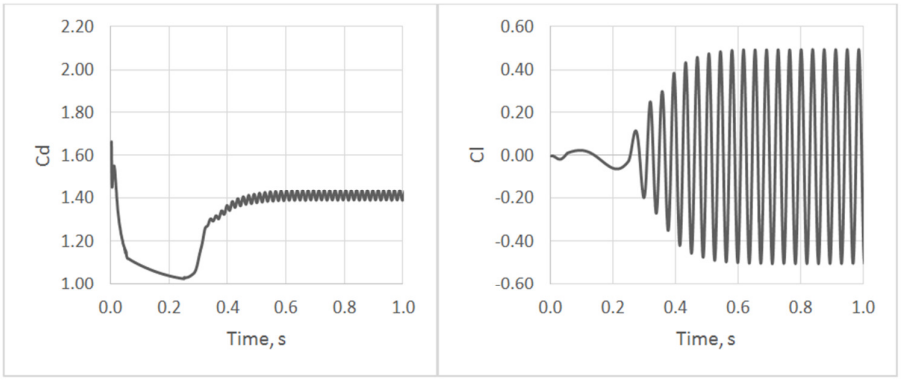

(b) Two interlocking squares

Fig. 3. Time history of Drag and Lift Coefficient at Re=150 for a) square cylinder; and b) two interlocking squares cylinder

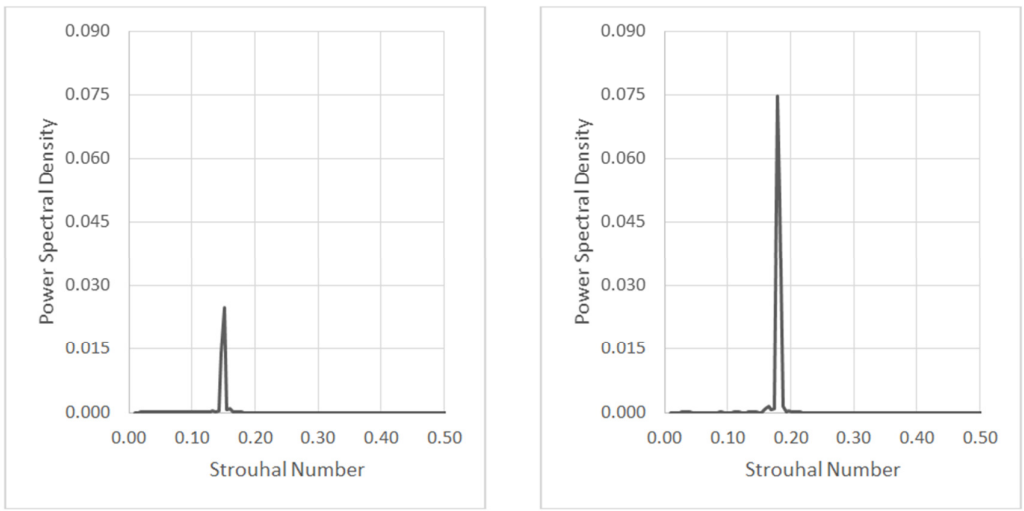

(a) Square Cylinder (b) Two Interlocking Square

Fig. 4. Power Spectral Density for a) square cylinder; and b) two interlocking squares cylinder

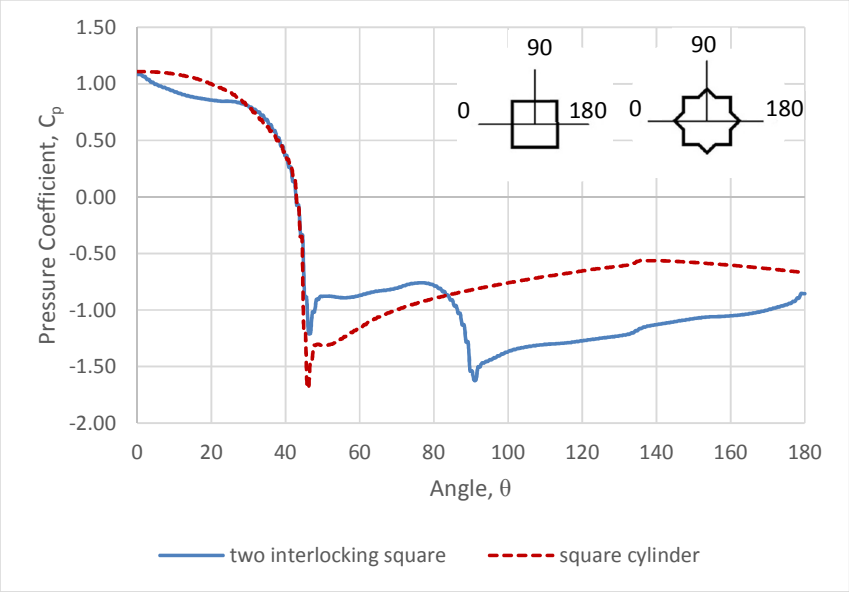

Fig. 5. Distribution of the pressure coefficient on the cylinder surfaces

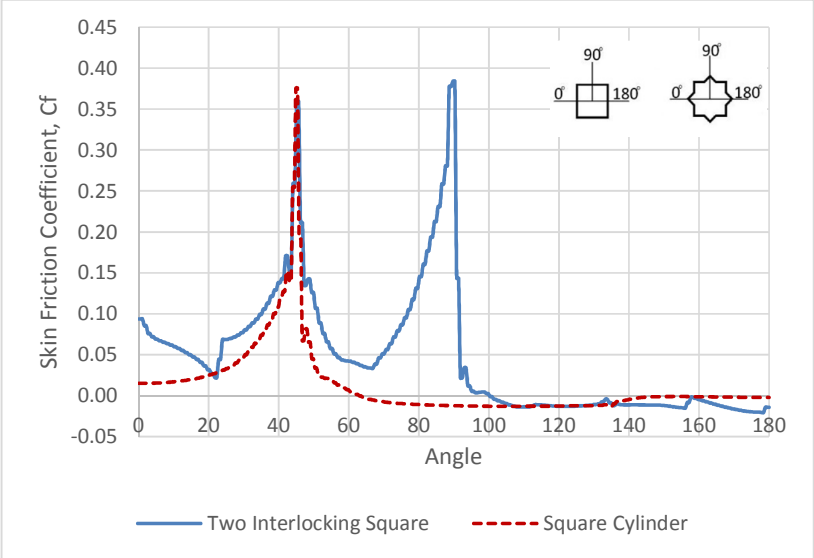

Fig. 6. Distribution of the skin friction coefficient on the cylinder surfaces

Figure 8 and 9 evidently shows the stagnation point at the leading edge of the square cylinder and also the two interlocking squares cylinder, consistent with the pressure contours. Figure 9 shows that the flow recirculates behind both cylinders with early interaction between the two shear layers is observed behind the interlocking squares cylinder wake due to the flow separation that occur at 100°. This is in contrast to the square cylinder wake where the flow separates early at 64° resulting in a slightly large lateral distance between the two shear layers that delay their interactions.

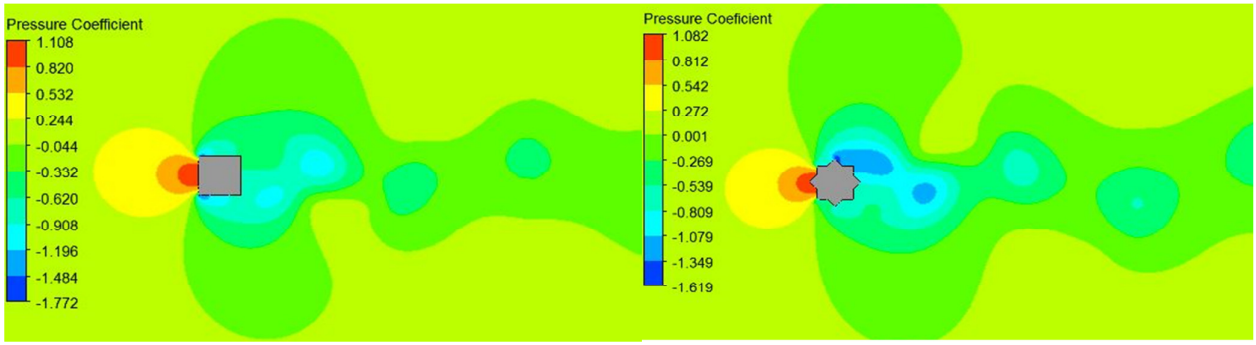

Square Cylinder Two Interlocking Square

Fig. 7. Pressure Coefficient contour for square cylinder and two interlocking squares cylinder

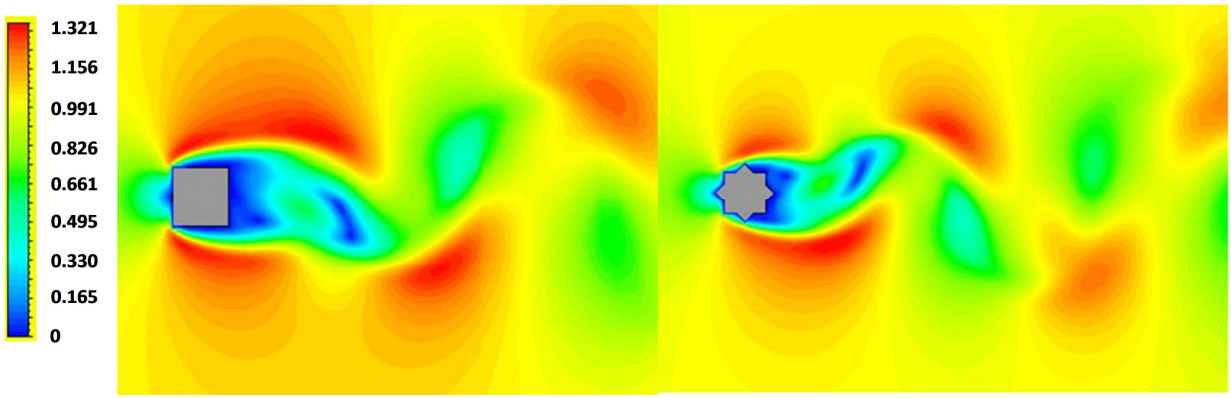

Square Cylinder Two Interlocking Squares

Fig. 8. Normalized velocity contour for square cylinder and two interlocking squares cylinder

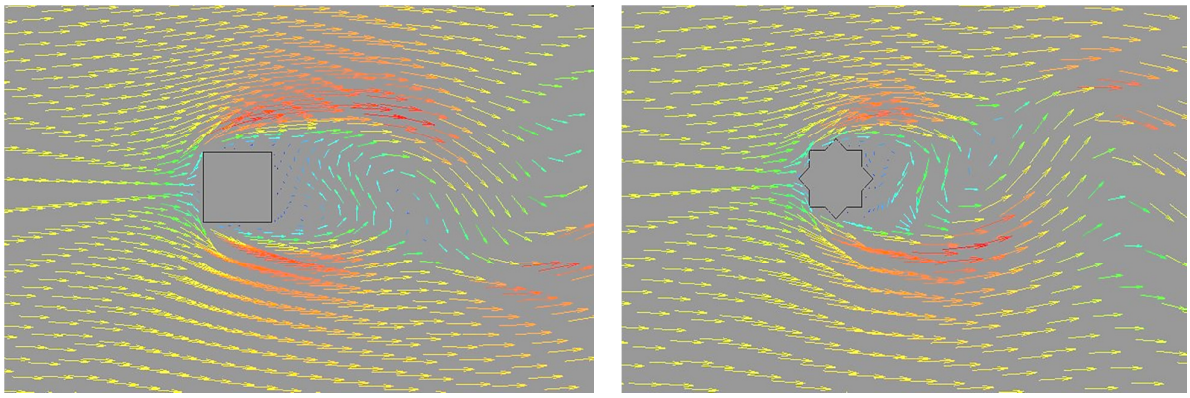

Square Cylinder Two Interlocking Square

Fig. 9. Velocity vector for square cylinder and two interlocking squares cylinder

Figure 10 displays the vorticity contours at an instant of time where both flows are characterized by a great alternating vortex shedding where the negative vorticity is shown in blue and positive vorticity is shown in red. Maximum magnitude of vorticity concentration in the two interlocking squares cylinder wake is 6% higher than that of the square cylinder, hence, stronger

vortices is observed in the former than that in the latter. The lateral distance between the centers of the two vortices in the wake region of the two interlocking square is closer, i.e. vortex occur frequently in comparison to the square cylinder, consistent with the Strouhal number results. As the vortex moves further downstream, it starts to decay gradually in the two interlocking squares cylinder wake but decay rapidly in the square cylinder wake indicated by the fading vorticity contours. This result is also consistent with the pressure contour plots in Fig. 7.

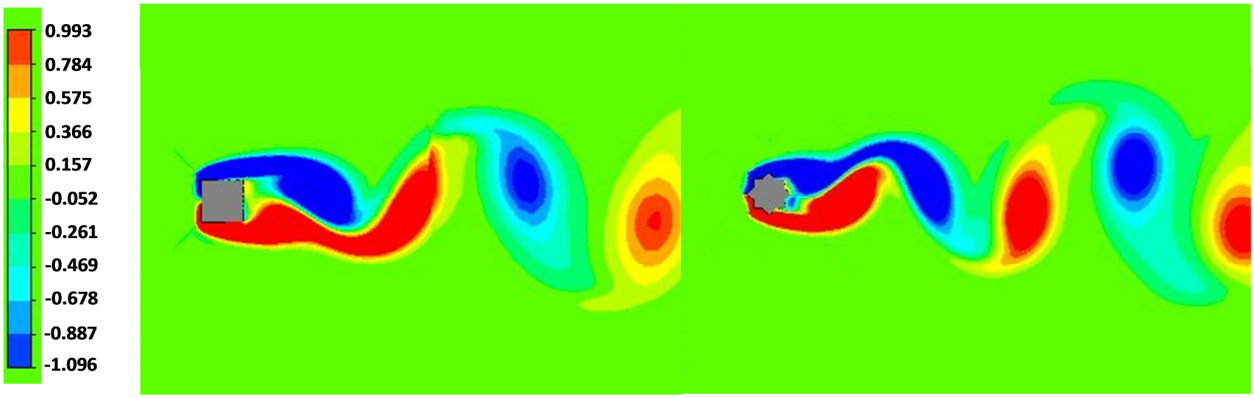

Fig. 10. Normalized instantaneous vorticity contour for square cylinder and two interlocking squares cylinder

4. Conclusions

CFD simulations of 2-D laminar flow over two interlocking squares cylinder at Reynolds number of 150 were performed and results were compared with that of a square cylinder. The computed results showed that the separation point occurred at a location 100º from the stagnation point, causing the shear layers to interact early in the wake of the two interlocking squares cylinder. Stronger vortices of higher frequency were observed behind the two interlocking squares cylinder where vortex decayed gradually in the streamwise direction in comparison to that of the square cylinder, hence producing large amplitude and fluctuations in the lift. This study demonstrate the potential of harvesting energy from this body as an alternative to the canonical body of a plain circular cylinder due to its nature of vortex shedding.

Acknowledgement

This work was supported by the Universiti Teknologi MARA, Malaysia under 600-IRMI/PERDANA 5/3 BESTARI (077/2018) Grant Scheme).

References

[1] Jan, Syed Aftab Alam, Farhad Ali, Nadeem Ahmad Sheikh, Ilyas Khan, Muhammad Saqib, and Madeha Gohar. "Engine oil based generalized brinkman-type nano-liquid with molybdenum disulphide nanoparticles of spherical shape: Atangana-Baleanu fractional model." *Numerical Methods for Partial Differential Equations* (2017).

[2] Bearman, P. W. "Circular cylinder wakes and vortex-induced vibrations." *Journal of Fluids and Structures* 27, no. 5-6 (2011): 648-658.

[3] Tamura, Tetsuro, and Tetsuya Miyagi. "The effect of turbulence on aerodynamic forces on a square cylinder with various corner shapes." *Journal of Wind Engineering and Industrial Aerodynamics* 83, no. 1-3 (1999): 135-145.

[4] Miran, Sajjad, and Chang Hyun Sohn. "Numerical study of the rounded corners effect on flow past a square cylinder." *International Journal of Numerical Methods for Heat & Fluid Flow* 25, no. 4 (2015): 686-702.

[5] Jue, Tswen-Chyuan. "Numerical analysis of vortex shedding behind a porous square cylinder." *International Journal of Numerical Methods for Heat & Fluid Flow* 14, no. 5 (2004): 649-663.
[6] Dutta, Sushanta, P. K. Panigrahi, and K. Muralidhar. "Experimental investigation of flow past a square cylinder at an angle of incidence." *Journal of engineering mechanics* 134, no. 9 (2008): 788-803.
[7] Yoon, Dong-Hyeog, Kyung-Soo Yang, and Choon-Bum Choi. "Flow past a square cylinder with an angle of incidence." *Physics of fluids* 22, no. 4 (2010): 043603.
[8] Dey, Prasenjit, and Ajoy Kr Das. "Numerical analysis of drag and lift reduction of square cylinder." *Engineering Science and Technology, an International Journal* 18, no. 4 (2015): 758-768.
[9] Chauhan, Manish Kumar, Sushanta Dutta, Bhupendra Singh More, and Bhupendra Kumar Gandhi. "Experimental investigation of flow over a square cylinder with an attached splitter plate at intermediate reynolds number." *Journal of Fluids and Structures* 76 (2018): 319-335.
[10] Abdelkefi, Abdessattar. "Aeroelastic energy harvesting: A review." *International Journal of Engineering Science* 100 (2016): 112-135.
[11] Rostami, Ali Bakhshandeh, and Mohammadmehdi Armandei. "Renewable energy harvesting by vortex-induced motions: Review and benchmarking of technologies." *Renewable and Sustainable Energy Reviews* 70 (2017): 193-214.
[12] Wells, Matthew. *Skyscrapers: Structure and design*. Laurence King Publishing, 2005.
[13] Robichaux, J., S. Balachandar, and S. P. Vanka. "Three-dimensional Floquet instability of the wake of square cylinder." *Physics of Fluids* 11, no. 3 (1999): 560-578.
[14] Inoue, O., Wakana Iwakami, and N. Hatakeyama. "Aeolian tones radiated from flow past two square cylinders in a side-by-side arrangement." *Physics of Fluids* 18, no. 4 (2006): 046104.
[15] Doolan, Con J. "Flat-plate interaction with the near wake of a square cylinder." *AIAA journal* 47, no. 2 (2009): 475-479.
[16] Ali, Mohamed Sukri Mat, Con J. Doolan, and Vincent Wheatley. "Low Reynolds number flow over a square cylinder with a detached flat plate." *International Journal of Heat and Fluid Flow* 36 (2012): 133-141.